



# Modified-ZrO<sub>2</sub> Supported Bimetallic Ruthenium-Tin Catalysts for Selective Hydrogenolysis of Furfuryl Alcohol to 1,5-Pentanediol

Thea Seventina Desiani Bodoi <sup>1,2</sup>, Ikhsan Mustari <sup>2</sup>, Anggita Nurfitriani <sup>2</sup>, Arif Ridhoni <sup>2</sup>, Firza Almervanka <sup>2</sup>, Atina Sabila Azzahra <sup>2,3</sup>, Utami Irawati <sup>1</sup>, Rodiansono <sup>1,2,\*</sup>



<sup>1</sup> Department of Chemistry, Faculty of Mathematics and Natural Sciences, Lambung Mangkurat University, Banjarbaru, Indonesia

<sup>2</sup> Catalysis for Sustainable Energy and Environment (CATSuRe), Inorganic Materials and Catalysis (IMCat) Laboratory, Lambung Mangkurat University, Banjarbaru, Indonesia

<sup>3</sup> School of Chemistry, Joseph Black Building, University of Glasgow, Glasgow, G12 8QQ, United Kingdom

\* Corresponding author: [rodiansono@ulm.ac.id](mailto:rodiansono@ulm.ac.id)

<https://doi.org/10.14710/jksa.29.1.64-72>

## Article Info

### Article history:

Received: 30<sup>th</sup> July 2025

Revised: 15<sup>th</sup> January 2026

Accepted: 17<sup>th</sup> January 2026

Online: 07<sup>th</sup> February 2026

### Keywords:

bimetallic Ru-Sn catalyst;  
modified-ZrO<sub>2</sub>; furfuryl alcohol;  
1,5-pentanediol

## Abstract

Biomass-derived platform C5-furanic compounds such as furfural (FFald) and furfuryl alcohol (FFalc) can be converted into 1,5-pentanediol (1,5-PeD), an important intermediate for textiles and plastics, via catalytic hydrogenolysis reaction. However, catalyst selectivity for the hydrogenolysis reaction of FFalc to 1,5-PeD remains a challenge. In this study, modification of ZrO<sub>2</sub> with metal oxides such as TiO<sub>2</sub>(R), TiO<sub>2</sub>(A), g-Al<sub>2</sub>O<sub>3</sub>, and active carbon (C) as the supports of bimetallic ruthenium-tin (Ru-Sn) catalysts for the selective hydrogenolysis of furfuryl alcohol (FFalc) to 1,5-pentanediol (1,5-PeD) has been investigated systematically. The modified-ZrO<sub>2</sub> supports were prepared by physical mixing using oxalic acid as a binder at room temperature, followed by calcination under N<sub>2</sub> at 300°C (ramping 2.5°C min<sup>-1</sup>) for 2 h. The supported Ru-Sn catalysts were synthesised by using the coprecipitation-hydrothermal method at 150°C for 24 h and reduced with H<sub>2</sub> at 400°C (ramping 3.3°C min<sup>-1</sup>) for 2 h. The synthesised catalysts were characterised by means of XRD, H<sub>2</sub>-TPR, and NH<sub>3</sub>-TPD. The pristine structures of ZrO<sub>2</sub>, TiO<sub>2</sub>, and g-Al<sub>2</sub>O<sub>3</sub> were maintained during the preparation of catalysts. Ru-Sn/ZrO<sub>2</sub>-TiO<sub>2</sub>(A) catalyst (Ru = 4 wt%, Sn = 1.30 wt%, ZrO<sub>2</sub> = 67 wt%, and TiO<sub>2</sub> (A) = 33 wt%) with calcination temperature of 300°C gave the highest yield of 1,5-PeD (72%) at 140°C, H<sub>2</sub> 10 bar for 3 h.

## 1. Introduction

The catalytic conversion of biomass feedstocks into fuels and chemicals via green chemistry and green economy approaches has been identified as the sustainable biomass-biorefinery [1, 2]. Lignocellulosic biomass consisted of lignin, cellulose, and hemicellulose, which can be converted into a variety of derived compounds such as substituted aromatics, phenol, reduced C5-C6 sugars, aldehydes, ketones, and organic acids. Furfural (FFald) is one of the important platform chemicals that can be produced by multiple acidic dehydration of C5-C6 sugars in cellulose or hemicellulose [3, 4]. Downstream upgrading of FFald via selective hydrogenation of FFald in the presence of heterogeneous transition metal catalysts produced furfuryl alcohol

(FFalc) and tetrahydrofurfuryl alcohol (THFalc) [5, 6]. The selective hydrogenolysis of furan ring in FFald, FFalc, and THFalc using supported transition metal catalysts produced a,w-diol (1,2-,1,4-,1,5-pentanediol (PeD)), which had been identified as the substituted 1,6-hexanediol (1,6-HeD) or 1,4-butanediol (1,4-BeD) in the polyester or polyurethane productions [7]. Commercially, 1,5-PeD was produced from a fossil-based precursor via multi-step reactions of glutaric acid using homogeneous catalysts [8]. Although the heterogeneous noble transition metal-based (e.g., Pt, Pd, Rh, Au, and Ir) catalysts have been intensively investigated for the synthesis of a,w-diol, the mixture of 1,5-PeD and 1,2-PeD products was inevitably obtained [9, 10, 11]. The proposed reaction pathways for the formation of a,w-diol from FFald and its derivatives are shown in Figure 1.

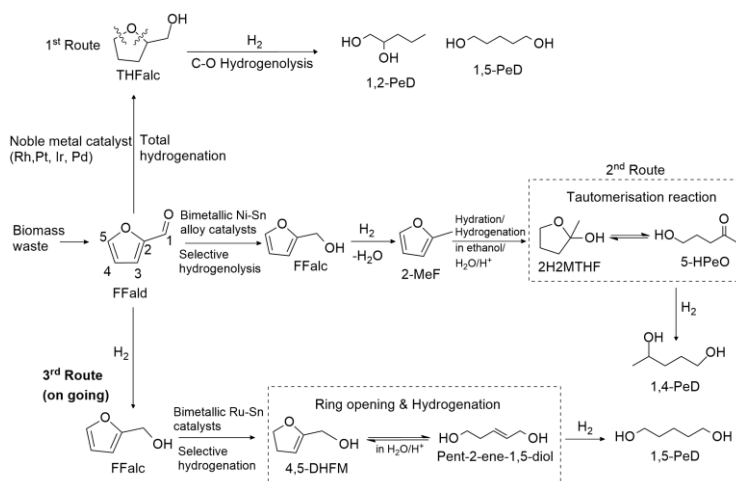


**Figure 1.** Proposed reaction pathways for the formation of a,w-diols from FFald using heterogeneous transition metal catalysts [12, 13, 14]

There are three proposed reaction routes for the transformation of FFald to a,w-diols. The 1<sup>st</sup> route is the common route, in which the first reaction is the hydrogenation of C=C and C=O bonds of FFald or FFalc to form THFalc under a hydrogen atmosphere. The saturated furan ring is hydrogenolysed over noble metal-based catalysts to form 1,2-PeD and 1,5-PeD, depending on the C-O bond cleavage of THFalc, reaction conditions, and catalysts. However, the selectivity of 1,5-PeD over 1,2-PeD from FFald or FFalc conversion remains inadequate.

There are three approaches for enhancing the selectivity of 1,5-PeD using catalysts; first, by addition of oxophilic metal oxides (e.g., MoO<sub>x</sub>, Y<sub>2</sub>O<sub>3</sub>, or WO<sub>x</sub>) into the active metal [15, 16], second, by the dispersion of the active metal within an acidic support and hydrothermally stable condition [17, 18], and third, the addition of an electropositive metal or promotor (e.g., Sn, In, Cu, Fe) in combination with an acidic support [13, 14]. The synergy between the active metal and the promoter is an important factor in increasing selectivity towards 1,5-PeD. For example, the Ni-Y<sub>2</sub>O<sub>3</sub> catalyst system produced a 42% yield of 1,5-PeD from FFalc at 150°C, with an initial H<sub>2</sub> pressure of 20 bar, after 24 h [15]. The ReO<sub>x</sub>-modified Rh/SiO<sub>2</sub> (Rh-ReO<sub>x</sub>/SiO<sub>2</sub>) catalysts selectively hydrogenolysed the C<sub>2</sub>-O bond of THFalc to produce 56% yield of 1,5-PeD at 60% conversion at 120°C, with an initial H<sub>2</sub> pressure of 80 bar, after 4 h [19]. Other combination catalyst systems, such as Pd-Ir-ReO<sub>x</sub>/SiO<sub>2</sub>, Rh-ReO<sub>x</sub>, and Rh-Ir-ReO<sub>x</sub> catalysts, were investigated for the conversion of FFald or FFalc to produce 1,5-PeD (78-80% yields) at 100-120°C, with an initial H<sub>2</sub> pressure of 60-80 bars, after 24 h [20, 21]. Another catalyst, such as an expensive metal, such as platinum (Pt) in Pt@Co<sup>2+</sup> catalyst, had produced a 47% yield of a,w-diols (27% 1,5-PeD and 20% 1,2-PeD) at 100% conversion of FFalc at 150°C, initial H<sub>2</sub> pressure of 30 bar, and after 4 h [22].

However, most reported catalyst systems require relatively harsh reaction conditions, while achieving precise control over product selectivity remains challenging. Therefore, improving the selectivity of 1,5-PeD under milder reaction conditions is an important

challenge for enhancing the sustainability of biomass-based diol production.

The 2<sup>nd</sup> route is the combination of selective-hydrolysis hydrogenation and furan ring tautomerisation reactions using bimetallic Ni-Sn alloy catalysts in ethanol/H<sub>2</sub>O phase to produce 1,4-PeD from FFald, FFalc, or 2-methylfuran (2-MeF). The synergistic actions between RANEY®Ni-Sn and ethanol/H<sub>2</sub>O involved the partial hydrogenation of C=C and the tautomerisation of reactions simultaneously to exclusively produce 1,4-pentanediol [23, 24]. In contrast to RANEY®Ni-Sn catalyst, bimetallic Ru-Sn catalysts have been explored as an alternative system for the selective production of 1,5-PeD from FFalc in the aqueous phase (Figure 1, 3<sup>rd</sup> route).

Bimetallic Ru-Sn catalysts supported on metal oxide supports (e.g., g-Al<sub>2</sub>O<sub>3</sub>, ZrO<sub>2</sub>, TiO<sub>2</sub> anatase (A), TiO<sub>2</sub> rutile (R), and charcoal (C)), have been investigated for this reaction. Previous studies have reported that the Ru-Sn catalyst supported on various metal oxides can promote a distinct reaction route [13, 14]. In this reaction route, 4,5-dihydromethylfuran methanol (4,5-DHFM) was identified as an intermediate from partial hydrogenation on the C=C, followed by C<sub>2</sub>-O bond cleavage of the furan ring in FFalc to produce 1,5-PeD during aqueous phase reaction [13, 25]. Therefore, the formation of 1,5-PeD highlights the roles of Ru-Sn active sites and surface acidity of the support.

For instance, Ru-Sn/g-Al<sub>2</sub>O<sub>3</sub>-TiO<sub>2</sub>(A) catalyst has been reported to produce high yields of 1,5-PeD (80%) at 180°C, 10 bar H<sub>2</sub> for 3 h [14]. Although Ru-Sn/g-Al<sub>2</sub>O<sub>3</sub>-TiO<sub>2</sub>(A) afforded the highest 1,5-PeD yield, ZrO<sub>2</sub> is chemically distinct from g-Al<sub>2</sub>O<sub>3</sub> in that it possesses amphoteric acid-base sites and stronger metal-support interactions, which have been reported to promote the hydrogenation reaction. Previous studies have demonstrated that the Ru/ZrO<sub>2</sub> catalyst exhibits better performance in the hydrogenation of levulinic acid into g-valerolactone in aqueous solvent [26]. Interestingly, the Ru-Sn/ZrO<sub>2</sub> catalyst also exhibited a high yield of 1,5-PeD (55%) at 180°C, with an initial H<sub>2</sub> pressure of 10 bar for 3 h, which is comparable to that of other supported bimetallic Ru-Sn catalysts [14].

In the present report, the extended investigations of  $\text{ZrO}_2$ -supported Ru-Sn catalysts for the selective hydrogenolysis of FFalc to 1,5-PeD under identical reaction conditions are described. The modification of  $\text{ZrO}_2$  with metal oxides (e.g.,  $\text{TiO}_2(\text{R})$ ,  $\text{TiO}_2(\text{A})$ ,  $\text{g-Al}_2\text{O}_3$ , and active carbon (C)) as the supports of bimetallic ruthenium-tin (Ru-Sn) catalysts was prepared and tested for the selective hydrogenolysis of FFalc to 1,5-PeD. The effects of support composition, calcination temperature, and reaction conditions on the yield of 1,5-PeD are also systematically discussed.

## 2. Experimental

### 2.1. Materials

$\text{RuCl}_3 \cdot x\text{H}_2\text{O}$  (Sigma-Aldrich, 99%),  $\text{SnCl}_2 \cdot 2\text{H}_2\text{O}$  (Sigma-Aldrich, 99%), charcoal (Sigma-Aldrich, 99%),  $\text{NaOH}$  (Sigma-Aldrich, 99%), 2-methoxy ethanol (Sigma-Aldrich, 99%), oxalic acid (Sigma-Aldrich, 99%), and ethanol (Sigma-Aldrich, 99,5%) for synthesis catalysts.  $\text{TiO}_2$  anatase and rutile (Guangzhou Hongwu Material Technology Co., Ltd, 99%),  $\text{g-Al}_2\text{O}_3$  (Merck Milipore, 99%),  $\text{ZrO}_2$  monoclinic (Wako Pure Chemical, 98%) for synthesis supports. Furfuryl alcohol (Sigma-Aldrich, 99%), dodecane (Sigma-Aldrich, 99%), 1,5-pentanediol (Tokyo Chemical Industry, 97%). Furfuryl alcohol as a reactant was purified using standard procedures prior to use [27].

### 2.2. Catalyst Preparation

#### 2.2.1. Preparation of Supports

The detailed procedure for synthesising  $\text{ZrO}_2\text{-TiO}_2$  (A) support is described as follows [28][29]:  $\text{ZrO}_2$  (0.6667 g) and  $\text{TiO}_2$  (anatase, 0.3333 g) were mixed at room temperature, and a 10 wt% oxalic acid solution was added dropwise until a homogeneous paste was formed. The paste was then dried at 110°C for 12 h and subsequently calcined at 300°C under an  $\text{N}_2$  flow of 100 mL/min for 2 h. The same procedure was applied to synthesize the other support.

#### 2.2.2. Preparation of Catalysts

A typical procedure for the synthesis of Ru-Sn/ $\text{ZrO}_2\text{-TiO}_2$  (A) (Ru = ~4 wt% and Sn = ~1.3 wt%) is described as follows [28][29]:  $\text{RuCl}_3 \cdot x\text{H}_2\text{O}$  was dissolved in deionised water (denoted as solution A), and  $\text{SnCl}_2 \cdot 2\text{H}_2\text{O}$  was dissolved in ethanol and 2-methoxy ethanol (denoted as solution B) at room temperature under gentle stirring. Solutions A, B, and 1.0 g of support ( $\text{ZrO}_2\text{-TiO}_2$  (A)) were mixed at room temperature. Then, the temperature was increased to 50°C, and the mixture was stirred for 12 h. The pH of the catalyst solutions was adjusted to 9-10 by adding an aqueous solution of  $\text{NaOH}$  (3.1 M) dropwise, and the solutions were transferred into a sealed Teflon autoclave reactor for hydrothermal processing at 150°C for 24 h. The obtained grey solid precipitate was washed with distilled water and ethanol. The precipitate was then dried *in vacuo* overnight. Prior to characterisation and catalytic reaction, Ru-Sn/ $\text{ZrO}_2\text{-TiO}_2$  (A) was reduced with  $\text{H}_2$  flow (100 mL/min) at 400°C for 2 h. The same procedure is used to synthesise other catalysts.

### 2.3. Catalyst Characterizations

The X-ray diffraction (XRD) analysis was performed using a Miniflex 600 Rigaku instrument with Cu as the monochromatic source of  $\text{CuK}\alpha$  radiation ( $\lambda = 0.1544 \text{ nm}$ ). The XRD was operated at 40 kV and 15mA with a step width of 0.02°, a scan speed at 4°  $\text{min}^{-1}$  ( $a_1 = 0.1540 \text{ nm}$ ,  $a_2 = 0.1544 \text{ nm}$ ), solar slit 1.25°, and a Ni  $\text{k}\beta$  filter.

Ammonia temperature-programmed desorption ( $\text{NH}_3\text{-TPD}$ ) was conducted on a ChemiSorb 2750 (Micromeritics). The samples were degassed at 10–200°C for 2 h to remove physisorbed gases prior to measurement. The temperature was then maintained at 350°C for 1 h while the sample was flushed with He gas.  $\text{NH}_3$  gas was introduced at 100°C for 30 min, then evacuated with helium (He) gas for 30 min to remove physisorbed  $\text{NH}_3$ . Finally, temperature-programmed desorption was conducted at a temperature of 100–800°C, and the desorbed  $\text{NH}_3$  was monitored by TCD.

The hydrogen temperature-programmed reduction ( $\text{H}_2\text{-TPR}$ ) was performed on a Chemisorb 2920 (Micromeritics). The samples were heated at 110°C for 60 min under a  $\text{N}_2$  stream with a flow rate of 50  $\text{mL min}^{-1}$ , then cooled to room temperature. Before the reduction processes, the line was purged with  $\text{H}_2$  (5% Ar gas v/v) for 30 min, then reduced with the same gas ( $\text{H}_2$  (5% Ar v/v)) at an elevated temperature of 30–800°C with a ramp rate of 10°C  $\text{min}^{-1}$ . The  $\text{H}_2$  uptake was calculated using the calibration curve ( $\text{H}_2$  gas; 10% Ar gas v/v, and flow rate of 50  $\text{mL min}^{-1}$ ).

The ATR-IR analysis of adsorbed pyridine was performed using a Bruker Diamond. The catalyst sample was placed in a glass-tube reactor and heated to 150°C under  $\text{N}_2$  flow for 1 h. Next, the spectrum of adsorbed species was obtained after the introduction of 2–3 drops of pyridine at room temperature, followed by heating at 150°C for 3 h with gentle stirring. After adsorption, the sample was evacuated to remove physisorbed pyridine and was monitored by ATR-IR spectroscopy on a Bruker Diamond at 400–4000  $\text{cm}^{-1}$ .

### 2.4. Catalytic Reactions

A typical catalytic reaction procedure is described as follows [13]: Catalyst (0.05 g), FFalc (0.0020 mol), n-dodecane as the internal standard (0.0002 mol), and  $\text{H}_2\text{O}$  (3 mL) were placed in a glass reaction tube, which was fitted into a stainless-steel reactor. The reactor was flushed with  $\text{H}_2$  at 2.5–5.0 bar approximately 30 times. After introducing an initial  $\text{H}_2$  pressure of 10 bar at room temperature, the reactor was heated to 160°C using a silicone oil heater equipped with a magnetic stirrer. After 3 h, the reaction mixture was transferred to a sample vial, centrifuged (~5000 rpm for 5 min), and analyzed by FID-GC (PerkinElmer). The catalyst was easily separated by centrifugation and then dried overnight under vacuum at room temperature before reusability testing.

### 2.5. Product Analysis

Analysis of reactants (FFalc) and product (1,5-PeD) was performed on a Perkin Elmer XL-Autosystem equipped with a flame ionisation detector (FID) and with

Restek Rtx@ BAC Plus 1 capillary column (30 m, 0.32 mmID, 1.8 mdf). GC analysis was performed at detector and injector temperatures of 240°C and 200°C, respectively, with N<sub>2</sub> as the carrier gas (14 mL min<sup>-1</sup>), and air and H<sub>2</sub> flow rates were 450 mL min<sup>-1</sup> and 38 mL min<sup>-1</sup>, respectively. The calibration curve was prepared using known concentrations of the internal standard (dodecane), the reactant, and commercially available products to determine the correct response factors, and was applied to calculate the analyte. The conversion of FFalc and the yield of the products were calculated using Equations (1) and (2).

$$\text{Conversion} = \frac{F_0 - F_t}{F_0} \times 100 \quad (1)$$

$$\text{Yield} = \frac{\text{mol product}}{F_0} \times \text{conversion of FFalc} \quad (2)$$

Where F<sub>0</sub> is the introduced mol reactant (FFalc), and F<sub>t</sub> is the remaining mol reactant, which are all obtained from GC analysis using an internal standard technique.

### 3. Results and Discussion

#### 3.1. Catalyst Characterization

The XRD patterns of three types of supported bimetallic Ru-Sn catalysts, c.a., Ru-Sn/ZrO<sub>2</sub>-TiO<sub>2</sub>(A), Ru-Sn/ZrO<sub>2</sub>-TiO<sub>2</sub>(R), and Ru-Sn/ZrO<sub>2</sub>-g-Al<sub>2</sub>O<sub>3</sub> after reduction with H<sub>2</sub> at 400°C for 2 h are shown in Figure 2(A). The pristine structures of ZrO<sub>2</sub> are observed at 2θ = 28.2°, 31.5°, 50.1°, and 59.8° (ICDD File No. 37-1484) [29]. The presence of ruthenium, tin, or Ru-Sn species cannot be detected by XRD due to the extremely low sample amount. The XRD patterns of supported Ru-Sn on ZrO<sub>2</sub>-TiO<sub>2</sub>(A) obtained after calcination at 300, 400, 500, and 600°C under N<sub>2</sub> for 2 h are shown in Figure 1(B). Figure 1(B) shows the presence of ZrO<sub>2</sub>-TiO<sub>2</sub>(A) support on Ru-Sn catalyst in all samples, a series of sharp diffraction peaks of TiO<sub>2</sub>(A) occurred at 2θ = 25.3°, 37.8°, 48.1°, 54.8°, 55.3°, and 62.9° (JCPDS card No. 21-1272) [30].

To further support the XRD data, the crystallite size of the Ru-Sn/ZrO<sub>2</sub>-TiO<sub>2</sub> (A) catalyst structure with varying calcination temperatures has been calculated using the Scherrer equation, specifically the TiO<sub>2</sub> (A) crystallite size. Based on the diffraction peak of TiO<sub>2</sub> (A) at 2θ = 25.3° in all samples, these peaks became sharper as the calcination temperature increased. The crystallite size of TiO<sub>2</sub> (A) at calcination temperatures of 300°C, 400°C, 500°C, and 600°C was estimated to be 15 nm, 17 nm, 19 nm, and 21 nm, respectively. This phenomenon is also observed in the Pt/TiO<sub>2</sub>-ZrO<sub>2</sub> catalyst [31].

The representative profile H<sub>2</sub>-TPR of Ru-Sn/ZrO<sub>2</sub>-TiO<sub>2</sub>(A) with H<sub>2</sub> uptake of 156.5 mmol/g is shown in Figure 3. An intensity reduction peak of RuO<sub>2</sub> to Ru<sup>0</sup> was observed at 95°C, suggesting the existence of RuO<sub>2</sub> interacting with the supports during the preparation of the catalyst [14]. The catalyst also shows a broad reduction peak at 227°C, as reported by Luo *et al.* [32] used a Ru<sub>3</sub>Sn<sub>7</sub> catalyst, indicating a shift in the reduction temperature of RuO<sub>2</sub> toward that of SnO<sub>2</sub> due to interaction between RuO<sub>2</sub> and SnO<sub>2</sub>. The reduction peak at 457°C indicates the typical reduction of SnO<sub>2</sub> species, which interact strongly with RuO<sub>2</sub>.

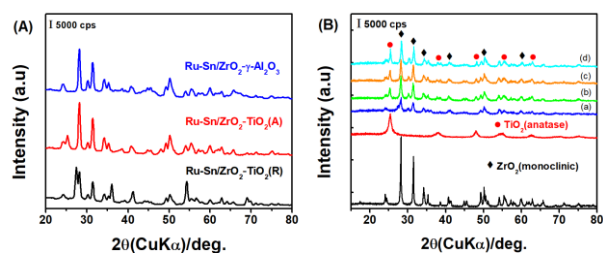


Figure 2. XRD patterns of (A) modified-ZrO<sub>2</sub> supported Ru-Sn, (B) supported Ru-Sn catalysts on ZrO<sub>2</sub>-TiO<sub>2</sub>(A) after calcination at different temperatures ((a) 300°C, (b) 400°C, (c) 500°C, and (d) 600°C)

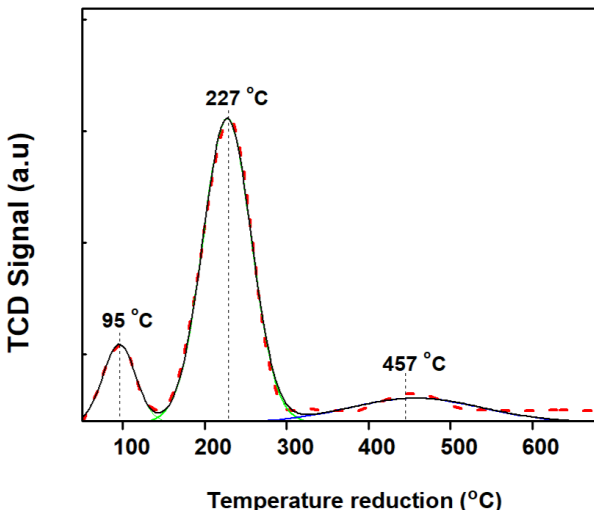


Figure 3. Representative H<sub>2</sub>-TPR profile of Ru-Sn/ZrO<sub>2</sub>-TiO<sub>2</sub>(A) catalyst after calcination with N<sub>2</sub> at 300°C for 2 h

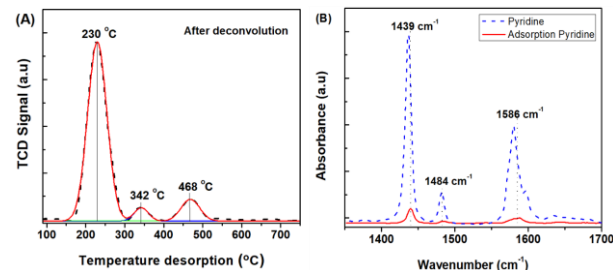


Figure 4. Representative of (A) NH<sub>3</sub>-TPD profile, and its deconvolution peaks, and (B) pyridine adsorption of Ru-Sn/ZrO<sub>2</sub>-TiO<sub>2</sub>(A) catalyst after reduction with H<sub>2</sub> at 400°C for 2 h

The NH<sub>3</sub>-TPD profiles were formally divided into three desorption temperature regions to denote three types of acid sites [33, 34]: (1) weak acid sites, ranging from 150–300°C, (2) medium acid sites, ranging from 300–500°C, and (3) strong acid sites, ranging from >500°C. The representative NH<sub>3</sub>-TPD profile of the Ru-Sn/ZrO<sub>2</sub>-TiO<sub>2</sub>(A) catalyst is shown in Figure 3(A). The Ru-Sn/ZrO<sub>2</sub>-TiO<sub>2</sub>(A) catalyst is dominated by weak acid sites at 230°C with an acidity of 350 mmol NH<sub>3</sub> per gram, accompanied by two small desorption peaks at 342°C, and 468°C as medium acid sites with an acidity of 61 mmol NH<sub>3</sub> per gram. Because NH<sub>3</sub>-TPD does not allow distinguishing Lewis and Brønsted acid sites, pyridine-ATR-IR analysis was performed on the representative of Ru-Sn/ZrO<sub>2</sub>-TiO<sub>2</sub>(A) catalyst, and the results are shown in Figure 4(B) and Table 1. Coordinatively bound NH<sub>3</sub> pyridine on Lewis acid sites shows bands around 1439

$\text{cm}^{-1}$  ( $\nu_{19b}$ ). Physisorbed or hydrogen-bonded pyridine shows a band around  $1586 \text{ cm}^{-1}$ . The band around  $1490 \text{ cm}^{-1}$  is common to vibrations due to  $\text{PyH}^+$  (Brønsted) and coordinatively bound pyridine (Lewis) [35].

### 3.2. Catalytic Reaction of Furfuryl Alcohol to 1,5-pantanediol

#### 3.2.1. Screening of Catalysts

Our previous research has shown that Ru-Sn catalysts combined with  $\gamma\text{-Al}_2\text{O}_3$ ,  $\text{TiO}_2$ (A), and  $\text{ZrO}_2$  can produce 1,5-PeD as the main product compared to other catalysts at  $180^\circ\text{C}$ , with an initial  $\text{H}_2$  pressure of 10–30 bar for 3–5 h. Interestingly,  $\text{g}\text{-Al}_2\text{O}_3$ ,  $\text{TiO}_2$  (A), and  $\text{ZrO}_2$  supported Ru-Sn catalysts afforded a high yield of 1,5-PeD were 69%, 55%, and 55%, respectively. In the experiment, the  $\text{g}\text{-Al}_2\text{O}_3$  support was modified with  $\text{TiO}_2$  (A) on the Ru-Sn catalyst, it was observed to enhance the production of 1,5-PeD by 80% at a conversion rate of 99% at  $180^\circ\text{C}$ , with an initial  $\text{H}_2$  pressure of 10 bar for 5 h [14].

In our recently published work, we evaluated the screening of a modified- $\text{ZrO}_2$ -supported bimetallic Ru-Sn catalyst in aqueous-phase hydrogenolysis of FFalc at  $160^\circ\text{C}$ , with an initial  $\text{H}_2$  pressure of 10 bar for 3 h. The results are summarised in Table 2. The Ru-Sn/ $\text{ZrO}_2$  catalysts gave 67% yield of 1,5-PeD as the main product, while yields of 4,5-DHFM (intermediate product) and levulinic acid (LA) were 28% and 5%, respectively, at 100% conversion of FFalc (Entry 1). Furthermore, using a charcoal (C)-modified  $\text{ZrO}_2$ -supported Ru-Sn catalyst slightly decreased the yields of 1,5-PeD (57%) and 4,5-DHFM (24%), but increased yields of CPO (4%) and other products (15%) (Entry 2). Furthermore,  $\text{ZrO}_2\text{-g}\text{-Al}_2\text{O}_3$  supported Ru-Sn catalyst gave 62% yield of 1,5-PeD with small amounts of CPO (2%) and THFalc (8%) at 86% conversion of FFalc (Entry 3).

The Ru-Sn/ $\text{ZrO}_2\text{-TiO}_2$  catalysts were also prepared using two different  $\text{TiO}_2$  phases, anatase (A) and rutile (R), and evaluated for the same reaction. The Ru-Sn/ $\text{ZrO}_2\text{-TiO}_2$ (A) catalyst yielded 70% of 1,5-PeD and 15% of 4,5-DHFM at 98% conversion of FFalc (Entry 4). In contrast, the Ru-Sn/ $\text{ZrO}_2\text{-TiO}_2$ (R) catalyst was preferred for producing 4,5-DHFM (62%) with a lower yield of 1,5-PeD (38%) at  $160^\circ\text{C}$ , 10 bar  $\text{H}_2$  for 3 h (Entry 5). Interestingly, lowering the reaction temperature to  $140^\circ\text{C}$  using Ru-Sn/ $\text{ZrO}_2\text{-TiO}_2$ (A) catalyst, the yield of 1,5-PeD slightly increased to 72%, accompanied by 4,5-DHFM (17%) and LA (11%) (Entry 6). Additionally, the formation of LA was mainly observed over the Ru-Sn/ $\text{ZrO}_2$ , Ru-Sn/ $\text{ZrO}_2\text{-g}\text{-Al}_2\text{O}_3$ , and Ru-Sn/ $\text{ZrO}_2\text{-TiO}_2$ (A) catalysts. Therefore, it can be concluded that the best catalyst for hydrogenolysis of FFalc was the Ru-Sn/ $\text{ZrO}_2\text{-TiO}_2$ (A) catalyst, and the reaction temperature was  $140^\circ\text{C}$ . This temperature will be applied for the next catalytic reaction of FFalc over Ru-Sn/ $\text{ZrO}_2\text{-TiO}_2$ (A) catalyst with different compositions of  $\text{ZrO}_2\text{-TiO}_2$ (A) and temperature of calcination.

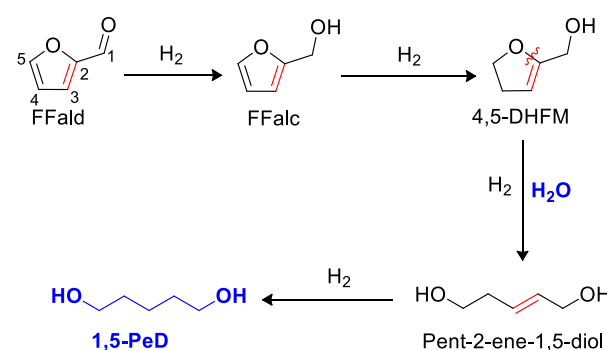


Figure 5. Proposed reaction pathways for selective hydrogenolysis of FFalc to 1,5-PeD over supported bimetallic Ru-Sn catalysts [13]

Table 1. Physico-chemical properties of the Ru-Sn/ $\text{ZrO}_2\text{-TiO}_2$  (A) catalyst

NH <sub>3</sub> -TPD (Acidity/μmol/g) <sup>a</sup>			Pyridine adsorption (band position)		
Weak (100–300°C)	Moderate (300–500°C)	Strong (>500°C)	Total acidity/μmol/g	Lewis acid	Brønsted acid
350	61	0	411	1439 $\text{cm}^{-1}$	-

<sup>a</sup>Total acidity was derived from NH<sub>3</sub>-TPD spectra

Table 2. Results of aqueous phase hydrogenolysis of FFalc using various modified- $\text{ZrO}_2$  supported Ru-Sn catalysts

Entry	Catalyst	Conv. (%)	Yields (%)					
			CPO	THFalc	4,5-DHFM	1,5-PeD	LA	Others
1	Ru-Sn/ $\text{ZrO}_2$	100	0	0	28	67	5	0
2	Ru-Sn/ $\text{ZrO}_2\text{-C}$	100	4	0	24	57	0	15
3	Ru-Sn/ $\text{ZrO}_2\text{-g}\text{-Al}_2\text{O}_3$	86	2	8	5	62	4	5
4	Ru-Sn/ $\text{ZrO}_2\text{-TiO}_2$ (A)	98	0	0	15	70	4	9
5	Ru-Sn/ $\text{ZrO}_2\text{-TiO}_2$ (R)	100	0	0	62	38	0	0
6 <sup>a</sup>	Ru-Sn/ $\text{ZrO}_2\text{-TiO}_2$ (A)	100	0	0	17	72	11	0

Reaction conditions: Cat. (0.05 g), FFalc (2.0 mmol),  $\text{H}_2\text{O}$  (3 mL),  $\text{H}_2$  (10 bar),  $160^\circ\text{C}$ , 3 h. <sup>a</sup>The condition reaction at  $140^\circ\text{C}$ , 10 bar  $\text{H}_2$  for 3 h.

**Table 3.** Results of aqueous phase hydrogenolysis of FFalc to 1,5-PeD, the different composition of  $\text{ZrO}_2\text{-TiO}_2\text{(A)}$  supports

Entry	Catalyst	Conv. (%)	Yields (%)				
			THFalc	4,5-DHFM	1,5-PeD	LA	Others
1	Ru-Sn/ $\text{ZrO}_2\text{-TiO}_2\text{(A)}$ (33%)	97	4	32	54	3	4
2	Ru-Sn/ $\text{ZrO}_2\text{-TiO}_2\text{(A)}$ (67%)	100	0	17	72	11	0
3	Ru-Sn/ $\text{ZrO}_2\text{-TiO}_2\text{(A)}$ (83%)	100	0	47	38	0	15

Reaction conditions: Cat. (0.05 g), FFalc (2.0 mmol),  $\text{H}_2$  (10 bar),  $140^\circ\text{C}$ , 3 h.

**Table 4.** Results of aqueous phase hydrogenolysis of FFalc to 1,5-PeD, the different calcination temperatures of  $\text{ZrO}_2\text{-TiO}_2\text{(A)}$  (67%) support

Entry	Catalyst	Conv. (%)	Yields (%)				
			THFalc	4,5-DHFM	1,5-PeD	LA	Others
1	Ru-Sn/ $\text{ZrO}_2\text{-TiO}_2\text{(A)}$ -300	100	0	17	72	11	0
2	Ru-Sn/ $\text{ZrO}_2\text{-TiO}_2\text{(A)}$ -400	100	2	40	27	15	16
3	Ru-Sn/ $\text{ZrO}_2\text{-TiO}_2\text{(A)}$ -500	99	0	25	65	4	5
4	Ru-Sn/ $\text{ZrO}_2\text{-TiO}_2\text{(A)}$ -600	100	0	0	0	0	100
5	Ru-Sn/ $\text{ZrO}_2\text{-TiO}_2\text{(A)}$ -300	99	0	40	40	7	12

Reaction conditions: Cat. (0.05 g), FFalc (2.0 mmol),  $\text{H}_2$  (10 bar),  $140^\circ\text{C}$ , 3 h.

To gain insight into the interaction between FFalc and the bimetallic Ru-Sn catalyst system, a general and plausible reaction mechanism has been proposed in Figure 5 based on previous studies [13]. Previous research on Ru-Sn/g-Al<sub>2</sub>O<sub>3</sub> catalysts has suggested that Ru species, Sn species, molecular water, and acidic supports play important roles in promoting partial hydrogenation of the C=C bond and cleavage of the C<sub>2</sub>-O bond of the furan ring in FFalc during aqueous-phase reactions. In the present Ru-Sn/ $\text{ZrO}_2\text{-TiO}_2\text{(A)}$  system, a similar reaction pathway is proposed for the formation of 1,5-PeD. Notably, 1,2-PeD was not detected, indicating that non-selective hydrogenation of the C-O cleavage pathways is suppressed. This phenomenon is likely associated with the interaction of Ru-Sn active sites and weak Lewis acid sites, which favor selective hydrogenation and controlled ring opening leading to 1,5-PeD. These results were also in accordance with the recent work of Rodiansono *et al.*, who reported the screening support of Ru-Sn catalysts for one-pot hydrogenolysis of FFalc to 1,5-PeD [13, 14, 25][29].

### 3.2.2. Effect of $\text{ZrO}_2\text{-TiO}_2\text{(A)}$ Composition

In order to get insight into the influence of  $\text{ZrO}_2\text{-TiO}_2\text{(A)}$  support, three types of supported Ru-Sn/ $\text{ZrO}_2\text{-TiO}_2\text{(A)}$ (x) catalysts with different compositions ( $\text{ZrO}_2$  to  $\text{TiO}_2\text{(A)}$ ), c.a. 33 wt%, 67 wt%, and 87 wt%, were prepared and evaluated for FFalc hydrogenolysis at  $140^\circ\text{C}$ , initial  $\text{H}_2$  pressure of 10 bar for 3 h. The results are summarised in Table 3.

The Ru-Sn/ $\text{ZrO}_2\text{-TiO}_2\text{(A)}$  (33%) catalyst gave 54% yield of 1,5-PeD, 4% THFA, 32% DHFM, 3% LA, and a small amount of other (typical dimer FFalc) at 97% conversion of FFalc (Entry 1). When the  $\text{ZrO}_2$  content increased to 67 wt%, the yield of 1,5-PeD increased to 72%, while that of 4,5-DHFM increased slightly to 17% at 100% conversion of FFalc (Entry 2). Further increasing the  $\text{ZrO}_2$  content to 83 wt% resulted in a significant

decrease in the 1,5-PeD yield to 38%. On the other hand, the yields of 4,5-DHFM and others (dimer-FFalc) increased two-fold to 47% and 15%, respectively (Entry 3). The increase of  $\text{ZrO}_2$  portion in  $\text{ZrO}_2\text{-TiO}_2\text{(A)}$  support may induce the ring opening reaction of the furan ring or dimerisation, as indicated by the increase in LA and dimer-FFalc. These products were generated due to the presence of Brønsted acid sites, as suggested by Rodiansono *et al.* [14]. Therefore, the subsequent investigation of this Ru-Sn/ $\text{ZrO}_2\text{-TiO}_2\text{(A)}$  (67%) was the effect of calcination temperatures.

### 3.2.3. Effect of Calcination Temperature

In an attempt to improve the yield of 1,5-PeD and to understand the  $\text{ZrO}_2\text{-TiO}_2\text{(A)}$ -x support in the catalyst system, the supported Ru-Sn catalyst was calcined with  $\text{N}_2$  at different temperatures, c.a.  $300^\circ\text{C}$ ,  $400^\circ\text{C}$ ,  $500^\circ\text{C}$ , and  $600^\circ\text{C}$  for 2 h, and the XRD patterns are shown in Figure 2(B). The results of the catalytic performance of these catalysts at  $140^\circ\text{C}$ , initial  $\text{H}_2$  pressure of 10 bar for 3 h, are summarised in Table 4.

The highest yield of 1,5-PeD (72%) was obtained over the Ru-Sn/ $\text{ZrO}_2\text{-TiO}_2$ -300 catalyst, while the yields of 4,5-DHFM and LA were 17% and 11%, respectively, at 100% conversion of FFalc (Entry 1). When the support was calcined at  $400^\circ\text{C}$ , the yield of 1,5-PeD decreased to 27%, whereas the yields of 4,5-DHFM and LA increased approximately threefold (40%) and 15%, respectively, at 100% conversion of FFalc (Entry 2). Furthermore, increasing the calcination temperature to  $500^\circ\text{C}$  slightly increased the yield of 1,5-PeD to 65% over the Ru-Sn/ $\text{ZrO}_2\text{-TiO}_2\text{(A)}$  catalyst after the support was calcined at  $500^\circ\text{C}$ .

A further increase in the calcination temperature to  $600^\circ\text{C}$  led to the formation of additional products, including 2-methylfuran (2-MeF), 2-pentanone (2-PeO), LA, and dimer-FFalc, with yields of 25%, 27%, 14%, and 34%, respectively (Entry 4). This phenomenon occurs

due to the increase in crystallinity of  $\text{TiO}_2$  at higher calcination temperature, which likely enhances strong metal-support interaction (SMSI) after the reduction [36]. Previous studies have reported that higher calcination and reduction temperatures promote encapsulation of Ru nanoparticle on  $\text{TiO}_2$ , particularly for the Ru/ $\text{TiO}_2$ -R system [37]. In this study, the crystallite size of  $\text{TiO}_2$  (A) calcined at 600°C was estimated to be 21 nm using the Scherrer equation. This increased crystallinity of  $\text{TiO}_2$  (A) is likely to reduce metal accessibility by partially covering active Ru-Sn sites and lowering hydrogenolysis activity. In addition, the reusability test was performed on the Ru-Sn/ $\text{ZrO}_2$ - $\text{TiO}_2$ (A)-300 catalyst, and the results are summarised in Table 4, Entry 5. The yield of 1,5-PeD was decreased to 40%, accompanied by increases in the yields of 4,5-DHFM (40%), LA (7%), and others (12%) (Entry 5). Therefore, the optimal calcination temperature for the  $\text{ZrO}_2$ - $\text{TiO}_2$  (A) support system was determined to be 300°C.

#### 4. Conclusion

Modification of  $\text{ZrO}_2$  with metal oxides such as  $\text{TiO}_2$ (R),  $\text{TiO}_2$ (A), g-Al<sub>2</sub>O<sub>3</sub>, and active carbon (C) as the supports of bimetallic ruthenium-tin (Ru-Sn) catalysts for the selective hydrogenolysis of furfuryl alcohol (FFalc) to 1,5-pentanediol (1,5-PeD) has been investigated systematically. The modified- $\text{ZrO}_2$  supports were prepared by physical mixing with oxalic acid as a binder at room temperature, followed by calcination under  $\text{N}_2$  at 300°C (ramping rate 2.5°C min<sup>-1</sup>) for 2 h. The supported Ru-Sn catalysts were synthesised by using the coprecipitation-hydrothermal method at 150°C for 24 h and reduced with  $\text{H}_2$  at 400°C (ramping 3.3°C min<sup>-1</sup>) for 2 h. The synthesised catalysts were characterised by XRD, H<sub>2</sub>-TPR, and NH<sub>3</sub>-TPD. The pristine structures of  $\text{ZrO}_2$ ,  $\text{TiO}_2$ , and g-Al<sub>2</sub>O<sub>3</sub> were maintained during the preparation of catalysts. The composition and calcination temperature of the  $\text{ZrO}_2$ - $\text{TiO}_2$  support significantly impacted the production of 1,5-PeD. Ru-Sn/ $\text{ZrO}_2$ - $\text{TiO}_2$ (A) with composition of  $\text{ZrO}_2$ - $\text{TiO}_2$  (A) 67% and calcination temperature of 300°C gave the highest yield of 1,5-PeD (72%) at 140°C,  $\text{H}_2$  10 bar for 3 h. The high activity and selectivity of Ru-Sn/ $\text{ZrO}_2$ - $\text{TiO}_2$ (A) catalyst can be attributed to the synergistic effect between the high dispersion of Ru or Ru-Sn nanoparticles and the presence of Lewis/Brønsted acid sites of the catalyst system. Further investigations into the catalyst-activity relationship over these Ru-Sn/ $\text{ZrO}_2$ - $\text{TiO}_2$ (A) catalysts for the hydrogenolysis of FFalc are in progress.

#### Acknowledgement

The authors acknowledge The Indonesian Endowment Funds for Education (LPDP) through BRIN-RIIM2 scheme (contract number of 79/IV/KS/11/2022), DRPTM-Kemendiktiainstek through Regular Fundamental scheme (contract number of 056/E5/PG.02.00.PL/2024), and LPPM-ULM through Internal Fundamental scheme (contract number of 1374.95/UN8.2/PG/2024 and 1878/UN8.2/PG/2025) for financial support. We also acknowledge the facilities, scientific and technical support from the Advanced

Chemical Characterization Laboratory, National Research and Innovation Agency, through E-Layanan Sains - BRIN.

#### References

- [1] Kui Wang, Jefferson William Tester, Sustainable management of unavoidable biomass wastes, *Green Energy and Resources*, 1, 1, (2023), 100005 <https://doi.org/10.1016/j.gerr.2023.100005>
- [2] Morgen Mukamwi, Tosin Somorin, Raimonda Soloha, Elina Dace, Databases for biomass and waste biorefinery – a mini-review and SWOT analysis, *Bioengineered*, 14, 1, (2023), 2286722 <https://doi.org/10.1080/21655979.2023.2286722>
- [3] Xiaodan Li, Pei Jia, Tiefeng Wang, Furfural: A Promising Platform Compound for Sustainable Production of C<sub>4</sub> and C<sub>5</sub> Chemicals, *ACS Catalysis*, 6, 11, (2016), 7621-7640 <https://doi.org/10.1021/acscatal.6b01838>
- [4] Xu Zhang, Siquan Xu, Qinfang Li, Guilin Zhou, Haian Xia, Recent advances in the conversion of furfural into bio-chemicals through chemo- and bio-catalysis, *RSC Advances*, 11, 43, (2021), 27042-27058 <https://doi.org/10.1039/D1RA04633K>
- [5] Rafael F. Perez, Marco A. Fraga, Hemicellulose-derived chemicals: one-step production of furfuryl alcohol from xylose, *Green Chemistry*, 16, 8, (2014), 3942-3950 <https://doi.org/10.1039/C4GC00398E>
- [6] Keiichi Tomishige, Yoshinao Nakagawa, Masazumi Tamura, Selective hydrogenolysis and hydrogenation using metal catalysts directly modified with metal oxide species, *Green Chemistry*, 19, 13, (2017), 2876-2924 <https://doi.org/10.1039/C7GC00620A>
- [7] Xiaobao Sun, Bin Wen, Feng Wang, Wenyu Zhang, Kangyu Zhao, Xianxiang Liu, Research advances on the catalytic conversion of biomass-derived furfural into pentanediols, *Catalysis Communications*, 187, (2024), 106864 <https://doi.org/10.1016/j.catcom.2024.106864>
- [8] Marcel Schlaf, Selective deoxygenation of sugar polyols to  $\alpha$ ,  $\omega$ -diols and other oxygen content reduced materials – a new challenge to homogeneous ionic hydrogenation and hydrogenolysis catalysis, *Dalton Transactions*, 39, (2006), 4645-4653 <https://doi.org/10.1039/B608007C>
- [9] David Martin Alonso, Stephanie G. Wettstein, James A. Dumesic, Bimetallic catalysts for upgrading of biomass to fuels and chemicals, *Chemical Society Reviews*, 41, 24, (2012), 8075-8098 <https://doi.org/10.1039/c2cs35188a>
- [10] O. G. Ellert, M. V. Tsodikov, S. A. Nikolaev, V. M. Novotortsev, Bimetallic nanoalloys in heterogeneous catalysis of industrially important reactions: synergistic effects and structural organization of active components, *Russian Chemical Reviews*, 83, 8, (2014), 718 <https://doi.org/10.1070/RC2014v08n08ABEH004432>
- [11] Keiichi Tomishige, Masayoshi Honda, Hiroshi Sugimoto, Lujie Liu, Mizuho Yabushita, Yoshinao Nakagawa, Recent progress on catalyst development for ring-opening C-O hydrogenolysis of cyclic ethers in the production of biomass-derived

chemicals, *Carbon Neutrality*, 3, 1, (2024), 17  
<https://doi.org/10.1007/s43979-024-00090-y>

[12] Rodiansono, Maria Dewi Astuti, Takayoshi Hara, Nobuyuki Ichikuni, Shogo Shimazu, One-pot selective conversion of C5-furan into 1,4-pentanediol over bulk Ni-Sn alloy catalysts in an ethanol/H<sub>2</sub>O solvent mixture, *Green Chemistry*, 21, 9, (2019), 2307-2315  
<https://doi.org/10.1039/C8GC03938K>

[13] Rodiansono, Atina Sabila Azzahra, Uripto Trisno Santoso, Edi Mikrianto, Eka Suarso, Kiky Corneliasari Sembiring, Indri Badria Adilina, Gagus Ketut Sunnardianto, Ahmad Afandi, Highly efficient and selective aqueous phase hydrogenolysis of furfural to 1,5-pentanediol using bimetallic Ru-SnO<sub>x</sub>/γ-Al<sub>2</sub>O<sub>3</sub> catalysts, *Catalysis Science & Technology*, 15, 3, (2025), 808-821  
<https://doi.org/10.1039/D4CY01138D>

[14] Rodiansono Rodiansono, Atina Sabila Azzahra, Edi Mikrianto, Arif Ridhoni, Ikhsan Mustari, Anggita Nurfitriani, Thea Seventina Desiani Bodoi, Rahmat Eko Sanjaya, Eka Suarso, Pathur Razi Ansyah, Screening Support of Bimetallic Ruthenium-Tin Catalysts for Aqueous Phase Hydrogenolysis of Furfuryl Alcohol to 1,5-Pentanediol, *Bulletin of Chemical Reaction Engineering & Catalysis*, 20, 2, (2025), 293-306  
<https://doi.org/10.9767/bcrec.20357>

[15] Husni Wahyu Wijaya, Takashi Kojima, Takayoshi Hara, Nobuyuki Ichikuni, Shogo Shimazu, Synthesis of 1,5-Pentanediol by Hydrogenolysis of Furfuryl Alcohol over Ni-Y<sub>2</sub>O<sub>3</sub> Composite Catalyst, *ChemCatChem*, 9, 14, (2017), 2869-2874  
<https://doi.org/10.1002/cctc.201700066>

[16] Rodiansono, Heny Puspita Dewi, Kamilia Mustikasari, Maria Dewi Astuti, Sadang Husain, Sutomo, Selective hydroconversion of coconut oil-derived lauric acid to alcohol and aliphatic alkane over MoO<sub>x</sub>-modified Ru catalysts under mild conditions, *RSC Advances*, 12, 21, (2022), 13319-13329  
<https://doi.org/10.1039/D2RA02103>

[17] Lungang Chen, Yulei Zhu, Hongyan Zheng, Chenghua Zhang, Yongwang Li, Aqueous-phase hydrodeoxygenation of propanoic acid over the Ru/ZrO<sub>2</sub> and Ru-Mo/ZrO<sub>2</sub> catalysts, *Applied Catalysis A: General*, 411-412, (2012), 95-104  
<https://doi.org/10.1016/j.apcata.2011.10.026>

[18] Jiajie Huo, Jean-Philippe Tessonner, Brent H. Shanks, Improving Hydrothermal Stability of Supported Metal Catalysts for Biomass Conversions: A Review, *ACS Catalysis*, 11, 9, (2021), 5248-5270  
<https://doi.org/10.1021/acscatal.1c00197>

[19] Shuichi Koso, Naoyuki Ueda, Yasunori Shimmi, Kazu Okumura, Tokushi Kizuka, Keiichi Tomishige, Promoting effect of Mo on the hydrogenolysis of tetrahydrofurfuryl alcohol to 1,5-pentanediol over Rh/SiO<sub>2</sub>, *Journal of Catalysis*, 267, 1, (2009), 89-92  
<https://doi.org/10.1016/j.jcat.2009.07.010>

[20] Sibao Liu, Yasushi Amada, Masazumi Tamura, Yoshinao Nakagawa, Keiichi Tomishige, One-pot selective conversion of furfural into 1,5-pentanediol over a Pd-added Ir-ReO<sub>x</sub>/SiO<sub>2</sub> bifunctional catalyst, *Green Chemistry*, 16, 2, (2014), 617-626  
<https://doi.org/10.1039/C3GC41335G>

[21] Sibao Liu, Yasushi Amada, Masazumi Tamura, Yoshinao Nakagawa, Keiichi Tomishige, Performance and characterization of rhenium-modified Rh-Ir alloy catalyst for one-pot conversion of furfural into 1,5-pentanediol, *Catalysis Science & Technology*, 4, 8, (2014), 2535-2549  
<https://doi.org/10.1039/C4CY00161C>

[22] A. Barranca, I. Gandarias, P. L. Arias, I. Agirrezabal-Telleria, One-Pot Production of 1,5-Pentanediol from Furfural Through Tailored Hydrotalcite-Based Catalysts, *Catalysis Letters*, 153, 7, (2023), 2018-2025  
<https://doi.org/10.1007/s10562-022-04144-7>

[23] Rodiansono, Maria Dewi Astuti, Kamilia Mustikasari, Sadang Husain, Pathur Razi Ansyah, Takayoshi Hara, Shogo Shimazu, Unravelling the one-pot conversion of biomass-derived furfural and levulinic acid to 1,4-pentanediol catalysed by supported RANEY® Ni-Sn alloy catalysts, *RSC Advances*, 12, 1, (2022), 241-250  
<https://doi.org/10.1039/D1RA06135F>

[24] Rodiansono, Atina Sabila Azzahra, Pathur Razi Ansyah, Sadang Husain, Shogo Shimazu, Rational design for the fabrication of bulk Ni<sub>3</sub>Sn<sub>2</sub> alloy catalysts for the synthesis of 1,4-pentanediol from biomass-derived furfural without acidic co-catalysts, *RSC Advances*, 13, 31, (2023), 21171-21181  
<https://doi.org/10.1039/D3RA03642A>

[25] Rodiansono, Atina Sabila Azzahra, Edi Mikrianto, Kiky Corneliasari Sembiring, Ahmad Afandi, Gagus Ketut Sunnardianto, Indri Badria Adilina, One-pot synthesis of confined structure Ru<sub>3</sub>Sn<sub>7</sub> alloys on alumina for exceptionally rapid and selective hydrogenolysis of furfuryl alcohol to 1,5-pentanediol, *Catalysis Science & Technology*, 15, 18, (2025), 5452-5463  
<https://doi.org/10.1039/D5CY00542F>

[26] Jamal Ftouni, Ara Muñoz-Murillo, Andrey Goryachev, Jan P. Hofmann, Emiel J. M. Hensen, Li Lu, Christopher J. Kiely, Pieter C. A. Bruijnincx, Bert M. Weckhuysen, ZrO<sub>2</sub> Is Preferred over TiO<sub>2</sub> as Support for the Ru-Catalyzed Hydrogenation of Levulinic Acid to γ-Valerolactone, *ACS Catalysis*, 6, 8, (2016), 5462-5472  
<https://doi.org/10.1021/acscatal.6b00730>

[27] Wilfred L. F. Armarego, *Purification of Laboratory Chemicals*, Butterworth-Heinemann, 2017,

[28] A. S. Azzahra, N. Annisa, R. Rodiansono, U. Trisno Santoso, R. Eko Sanjaya, E. Suarsa, Effect of Charcoal-Doping on The Yield of 1, 5-Pentanediol and Reusability in Ru-Sn/g-Al<sub>2</sub>O<sub>3</sub>-Charcoal Catalysts, *1st ICWSDGs2024*, 2025

[29] Onkar Mangla, Savita Roy, Monoclinic Zirconium Oxide Nanostructures Having Tunable Band Gap Synthesized under Extremely Non-Equilibrium Plasma Conditions, *Proceedings*, 3, 1, (2019), 10  
[https://doi.org/10.3390/IOCN\\_2018-1-05486](https://doi.org/10.3390/IOCN_2018-1-05486)

[30] Md Sahadat Hossain, Samina Ahmed, Easy and green synthesis of TiO<sub>2</sub> (Anatase and Rutile): Estimation of crystallite size using Scherrer equation, Williamson-Hall plot, Monshi-Scherrer Model, size-strain plot, Halder-Wagner Model, *Results in Materials*, 20, (2023), 100492  
<https://doi.org/10.1016/j.rinma.2023.100492>

[31] Fengbo Li, Tao Lu, Bingfeng Chen, Zhijun Huang, Guoqing Yuan, Pt nanoparticles over TiO<sub>2</sub>-ZrO<sub>2</sub>

mixed oxide as multifunctional catalysts for an integrated conversion of furfural to 1,4-butanediol, *Applied Catalysis A: General*, 478, (2014), 252-258 <https://doi.org/10.1016/j.apcata.2014.04.012>

[32] Zhicheng Luo, Qiming Bing, Jiechen Kong, Jing-yao Liu, Chen Zhao, Mechanism of supported  $\text{Ru}_3\text{Sn}_7$  nanocluster-catalyzed selective hydrogenation of coconut oil to fatty alcohols, *Catalysis Science & Technology*, 8, 5, (2018), 1322-1332 <https://doi.org/10.1039/C8CY00037A>

[33] J. C. Yori, J. M. Grau, V. M. Benítez, C. R. Vera, C. L. Pieck, J. M. Parera, Comparison between Ni and Pt promoted  $\text{SO}_4^{2-}-\text{ZrO}_2$  catalysts for *n*-octane hydroisomerization-cracking, *Catalysis Letters*, 100, 1, (2005), 67-71 <https://doi.org/10.1007/s10562-004-3087-8>

[34] Hanan Atia, Udo Armbruster, Andreas Martin, Dehydration of glycerol in gas phase using heteropolyacid catalysts as active compounds, *Journal of Catalysis*, 258, 1, (2008), 71-82 <https://doi.org/10.1016/j.jcat.2008.05.027>

[35] Masazumi Tamura, Ken-ichi Shimizu, Atsushi Satsuma, Comprehensive IR study on acid/base properties of metal oxides, *Applied Catalysis A: General*, 433-434, (2012), 135-145 <https://doi.org/10.1016/j.apcata.2012.05.008>

[36] Joby Sebastian, Chalachew Mebrahtu, Feng Zeng, Regina Palkovits, Strong Metal-Support Interactions on  $\text{TiO}_2$ -Supported Metal Catalysts for Fine-Tuning Catalysis, *Angewandte Chemie International Edition*, 65, 1, (2026), e02611 <https://doi.org/10.1002/anie.202502611>

[37] Yaru Zhang, Wenjie Yan, Haifeng Qi, Xiong Su, Yang Su, Xiaoyan Liu, Lin Li, Xiaofeng Yang, Yanqiang Huang, Tao Zhang, Strong Metal-Support Interaction of Ru on  $\text{TiO}_2$  Derived from the Co-Reduction Mechanism of  $\text{Ru}_x\text{Ti}_{1-x}\text{O}_2$  Interphase, *ACS Catalysis*, 12, 3, (2022), 1697-1705 <https://doi.org/10.1021/acscatal.1c04785>